

Contribution from the Department of Chemistry, University of California, Berkeley, California 94720, Department of Chemistry, University of Oslo, P.O. Box 1033, N-0315 Oslo 3, Norway, Inorganic Chemistry Laboratories, South Parks Road, Oxford OX1 9QR, Great Britain, and School of Chemistry and Molecular Sciences, University of Sussex, Brighton BN1 9QJ, Great Britain

Synthesis of Bis[bis(trimethylsilyl)amido]iron(II). Structure and Bonding in $M[N(\text{SiMe}_3)_2]_2$ ($M = \text{Mn, Fe, Co}$): Two-Coordinate Transition-Metal Amides

R. A. Andersen,*[†] Knut Faegri, Jr.,[‡] Jennifer C. Green,*[§] Arne Haaland,*[‡] M. F. Lappert,*^{||} Wing-Por Leung,^{||} and Kristin Rypdal[‡]

Received November 3, 1987

Bis[bis(trimethylsilyl)amido]iron(II), $\text{Fe}[N(\text{SiMe}_3)_2]_2$, has been prepared from $\text{FeBr}_2(\text{THF})_2$ and $\text{LiN}(\text{SiMe}_3)_2$. The corresponding Co(II) and Mn(II) amides are known to be dimeric in the crystalline phase, and the Co amide is known to be monomeric in freezing benzene. All three amides are monomeric in the gas phase at 130–150 °C/1 Torr. Gas electron diffraction data are consistent with monomers of S_4 symmetry (which implies $\angle \text{NMN} = 180^\circ$) and bond distances of Mn–N = 195 (2), Fe–N = 184 (2), and Co–N = 184 (2) pm. Intraligand strain is reduced by opening of the SiNSi angle to 130° and rotation of SiMe_3 groups. Comparison with the structures of the amido-bridged dimers of the Mn and Co amides shows that dimer formation is accompanied by significant elongation of the terminal M–N bonds and compression of the SiNSi valence angle of the terminal ligand by about 10°. Both changes are interpreted as evidence for ligand–ligand repulsion in the dimers. SCF MO calculations on high-spin 6A_1 $\text{Mn}(\text{NH}_2)_2$ yield an equilibrium bond distance of Mn–N = 193 pm. It is concluded that the monomeric Mn amide is high spin. The SCF calculations suggest that the Mn–N bonding is very polar and that N–Mn $p\pi$ – $d\pi$ bonding is negligible. The photoelectron (PE) spectra of the Mn and Fe amides have been recorded and assigned. The similarity of the PE spectra of the Fe and Co amides to that of the Mn analogue suggests (but does not prove) that these species are high-spin 2B_1 and 3A_2 , respectively.

Introduction

In recent years the structures of a series of monomeric main-group metal diamides $M[N(\text{SiMe}_3)_2]_2$, where $M = \text{Be},^1 \text{Mg},^2 \text{Zn},^3 \text{Cd},^4 \text{Hg},^5 \text{Ge},^6 \text{Sn},^7$ and Pb^6 and $\text{Me} = \text{CH}_3$, have been determined by gas electron diffraction (GED). The group 2 and 12 amides are isostructural, with a linear N–M–N backbone, and the Ge, Sn, and Pb diamides are bent, with $\angle \text{NMN}$ equal to 100° or less.

Structural information on molecules containing two-coordinate Mn, Fe, or Co is limited to gaseous dihalides⁸ and manganese dialkyls.⁹ The bis(trimethylsilyl)amides $M[N(\text{SiMe}_3)_2]_2$ ($M = \text{Mn, Co}$) were first synthesized by Bürger and Wannagat.^{10,11} Both compounds are dimeric (with bridging amido groups) in the crystalline phase.^{12,13} The Co amide is, however, monomeric in benzene solution (by cryoscopy) and in the gas phase (by mass spectrometry (MS)).¹⁴

We now report the synthesis of the Fe(II) amide $\text{Fe}[N(\text{SiMe}_3)_2]_2$ (by R.A.A.), the molecular structures of $M[N(\text{SiMe}_3)_2]_2$ ($M = \text{Mn, Fe, Co}$), as determined by GED, the photoelectron spectra of the Mn(II) and Fe(II) amides to supplement those previously published for $\text{Co}[N(\text{SiMe}_3)_2]_2$,¹⁵ and SCF MO calculations on high-spin (6A_1) $\text{Mn}(\text{NH}_2)_2$.

Experimental Section

Synthesis. All preparations were performed under an inert atmosphere.

$\text{Fe}[N(\text{SiMe}_3)_2]_2$. To $\text{FeBr}_2(\text{THF})_2$ (8.3 g, 0.023 mol) suspended in diethyl ether (80 mL) at 0 °C was added $\text{LiN}(\text{SiMe}_3)_2$ (0.8 M in OEt_2) (10.4 g, 0.0460 mol) in diethyl ether (100 mL), and the suspension was stirred for 12 h at 0 °C. Diethyl ether was removed under reduced pressure, and the brown-green residue was extracted with pentane (50 mL). The red solution was filtered, and the filtrate was taken to dryness, leaving a dark oil that was distilled as a green-yellow liquid at 80–90 °C/10^{−2} mm (bath temperature was 115–125 °C). The liquid solidified to a soft green-yellow solid at ca. 5 °C. The yield was 6 g (90%).

Infrared (IR) spectra were recorded as Nujol mulls between cesium iodide windows on a Perkin-Elmer 537 instrument: 1250 s, sh, 1240 s, 1175 w, 1020 m, sh, 990 s, 970 s, 845 s, 825 s, 783 m, 745 m, 700 w, 657 m, 628 w, 605 m, 355 s cm^{-1} . Electron impact mass spectra were recorded on an AEI-MS-12 instrument equipped with a direct inlet. M^+ m/e (calculated, found relative intensity): 376 (100, 100), 377 (36.8, 33.6), 378 (19.8, 17.3), 379 (4.93, 3.54).

$\text{Co}[N(\text{SiMe}_3)_2]_2$. This compound was prepared by a literature method,¹⁰ purified by vacuum sublimation at 50–70 °C/10^{−2} mm, and identified by MS and IR spectroscopy.¹⁴

$\text{Mn}[N(\text{SiMe}_3)_2]_2$. This compound was prepared by a modification of the literature method.^{11,12} Two equivalents of solid $\text{LiN}(\text{SiMe}_3)_2 \cdot \text{OEt}_2$ ¹⁷ was slowly added to a solution of MnCl_2 in thf. The mixture was stirred at ambient temperature for ca. 2 h. The solvent was removed in vacuo. The residue was heated at 120 °C in a stream of argon for 1 h and was then recrystallized from cold (−30 °C) pentane to afford the crystalline compound (mp 55–60 °C). The compound can be distilled at 112–120 °C/0.2 mm.

The electron impact mass spectrum showed it to be monomeric in the gas phase; the most intense m/e peak was that of the monomeric parent ion at m/e 375, with intense peaks at m/e 360 and 275. In *n*-pentane the compound is dimeric, according to the Signer method (m/e found, $M = 768$; the dimer requires $M = 750$).

Gas Electron Diffraction. The electron diffraction data were recorded on a Balzers Eldigraph KDG-2 instrument with nozzle temperatures corresponding to vapor pressures of about 1 Torr: about 130 °C for $M = \text{Fe}$ and Co and about 150 °C for $M = \text{Mn}$. Exposures were made with nozzle-to-plate distances of 50 and 25 cm. Photometer data from four to six plates from each set were processed by standard procedures. The molecular intensity curves obtained from each nozzle-to-plate distance were averaged but not connected. The curves extended from $s = 28.75$ to 151.25 nm^{-1} with increment $\Delta s = 1.25 \text{ nm}^{-1}$ (50 cm) and from $s = 30.0$ to 255.0 nm^{-1} with increment $\Delta s = 2.5 \text{ nm}^{-1}$ (25 cm).

Atomic scattering factors, $f'(s)$, were taken from Schäfer, Yates, and Bonham.¹⁸ The molecular intensities were modified by multiplication

- (1) Clark, A. H.; Haaland, A. *Acta Chem. Scand.* **1970**, *24*, 3024.
- (2) Fjeldberg, T.; Andersen, R. A. *J. Mol. Struct.* **1984**, *125*, 287.
- (3) Haaland, A.; Hedberg, K.; Power, P. P. *Inorg. Chem.* **1984**, *23*, 1972.
- (4) Aleya, E. C.; Fisher, K. J.; Fjeldberg, T. *J. Mol. Struct.* **1985**, *127*, 325.
- (5) Aleya, E. C.; Fisher, K. J.; Fjeldberg, T. *J. Mol. Struct.* **1985**, *130*, 263.
- (6) Fjeldberg, T.; Hope, H.; Lappert, M. F.; Power, P. P.; Thorne, A. J. *J. Chem. Soc., Chem. Commun.* **1983**, 639.
- (7) Lappert, M. F.; Power, P. P.; Slade, M. J.; Hedberg, L.; Hedberg, K.; Schomaker, V. *J. Chem. Soc., Chem. Commun.* **1979**, 369.
- (8) Hargittai, M. In *Stereochemical Applications of Gas-Phase Electron Diffraction*; Hargittai, I., Ed.; VCH: Deerfield Beach, FL; Part B; in press.
- (9) Buttrus, N. H.; Eaborn, C.; Hitchcock, P. B.; Smith, D. J.; Sullivan, A. C. *J. Chem. Soc., Chem. Commun.* **1985**, 1380. Andersen, R. A.; Haaland, A.; Rypdal, K.; Volden, H. V. *J. Chem. Soc., Chem. Commun.* **1985**, 1807.
- (10) Bürger, H.; Wannagat, U. *Monatsh. Chem.* **1963**, *94*, 1007.
- (11) Bürger, H.; Wannagat, U. *Monatsh. Chem.* **1964**, *95*, 1099.
- (12) Bradley, D. C.; Hursthouse, M. B.; Malik, K. M. A.; Mösel, R. *Transition Met. Chem. (Weinheim, Ger.)* **1978**, *3*, 253.
- (13) Murray, B. D.; Power, P. P. *Inorg. Chem.* **1984**, *23*, 4584.
- (14) Bradley, D. C.; Fisher, K. J. *J. Am. Chem. Soc.* **1971**, *93*, 2058.
- (15) For an overview of metal amides, see: Lappert, M. F.; Power, P. P.; Sanger, A. R.; Srivastava, R. C. *Metal and Metalloid Amides*; Horwood: Chichester, U.K., 1980.
- (16) Green, J. C.; Payne, M.; Seddon, E. A.; Andersen, R. A. *J. Chem. Soc., Dalton Trans.* **1982**, 887.
- (17) Lappert, M. F.; Singh, A.; Atwood, J. L.; Hunter, W. E. *J. Chem. Soc., Chem. Commun.* **1983**, 206.

[†] University of California.

[‡] University of Oslo.

[§] Oxford University.

^{||} University of Sussex.

Table I. Interatomic Distances, Rms Vibrational Amplitudes (l), and Valence Angles of $M[N(\text{SiMe}_3)_2]_2$ ($M = \text{Mn, Fe, Co, Zn}^3$) (Estimated Standard Deviations in Parentheses in Units of the Last Digit; Nonrefined Parameter Values in Brackets)

	Interatomic Distances/pm							
	M = Mn		M = Fe		M = Co		M = Zn	
	r_a	l	r_a	l	r_a	l	r_a	l
Bond Distances								
M-N	195 (2)	3.0 (27)	184 (2)	3.6 (25)	184 (2)	4.7 (30)	182 (1)	4.2 (25)
N-Si	171.8 (6)	[5.3]	172.3 (5)	[5.3]	173.0 (7)	[5.3]	172.8 (7)	[5.7]
Si-C	187.6 (6)	6.3 (6)	189.6 (6)	6.3 (6)	188.3 (8)	5.9	188.9 (6)	6.2
C-H	110.6 (5)	7.8 (6)	110.0 (5)	8.6 (6)	109.7 (5)	7.3 (7)	110.5 (4)	8.3 (5)
Nonbonded Distances								
M...Si	308	10 (1)	300	12 (1)	300	11 (1)	299	11 (5)
N...C ^a	294	[10.0]	300	[10.0]	298	[10.0]	303	[9.8]
Si...H	249	[12.4]	249	13 (1)	249	12 (1)	251	13 (1)
C...C ^b	307	[13.3]	305	[13.3]	304	[13.3]	300	[11.3]
Si...Si ^c	314	15 (6)	314	7 (1)	314	7 (2)	314	[8.2]
M...C	313	47 (10)	316	38 (6)	316	24 (7)	330	15
M...C	418	25 (5)	421	35 (10)	415	45 (19)	to	to
M...C	458	11 (2)	450	15 (3)	453	12 (2)	454	30
Si...Si ^d	574	27 (6)	557	20 (3)	558	24 (5)	556	12
Angles/deg								
	M = Mn		M = Fe		M = Co		M = Zn	
Valence Angles								
$\angle \text{NMN}$	[180]		[180]		[180]		[180]	
$\angle \text{MNSi}$	114.0 (6)		114.4 (5)		144.7 (7)		114.8 (11)	
$\angle \text{SiNSi}$	132.1 (12)		131.2 (10)		130.6 (14)		130.4 (22)	
$\angle \text{NSiC}$	110 (1)		112 (1)		111 (1)		113 (2)	
$\angle \text{SiCH}$	111 (1)		109 (1)		111 (1)		111.1 (2)	
Torsion and Tilt Angles								
$\phi(\text{N-Si})$	17 (1)		13 (1)		18 (2)		20 (6)	
$\phi(\text{Si-C})$	[10]		[10]		[10]		[0]	
τ	[2]		[2]		[2.5]		[0]	

^a Mean value. ^b Within a SiMe_3 group. ^c Intraligand. ^d Interligand.

Table II. Ionization Energies (eV) for $M[N(\text{SiMe}_3)_2]_2$ ($M = \text{Mn, Fe, Co}$)

	band							
	X	A	B	C	D	E	F	G
Mn	7.9	8.5	9.1	10.3	11.4	13.8	15.3	21.4
Fe	8.0	8.5	9.2	10.3	11.3	13.7	15.9	21.3
Co ^a	8.1	8.6	9.6	10.3	11.5	13.2		19.6
assignt	d	N:	M-N	C-Si	N-Si	C-H	Si(3s)	C(2s)

^a From ref 16.

with $s/|f'_M||f'_N|$.

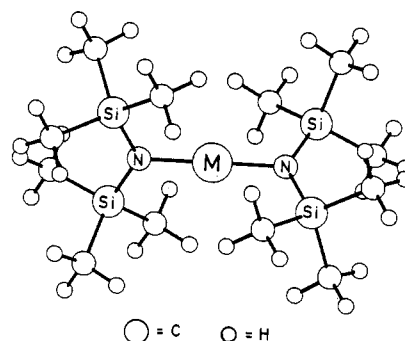
Structure Refinement. Structure refinements by least-squares calculations on the intensity data were based on models of S_4 symmetry as shown in Figure 1. A structure is then determined by the bond distances M-N, N-Si, Si-C, and C-H, the valence angles $\angle \text{MNSi}$, $\angle \text{NSiC}$, and $\angle \text{SiCH}$, and a torsion angle defining the angle of rotation of the SiMe_3 groups about the N-Si bond, $\phi(\text{N-Si})$. This angle was defined as zero when the overall molecular symmetry is D_{2d} .

Attempts were also made to refine a SiMe_3 tilt angle τ , defined as the angle between the C_3 symmetry axis of the SiMe_3 group and the Si-N bond, and a dihedral angle $\phi(\text{Si-C})$, defining the methyl group orientation. After some trial and error $\phi(\text{Si-C})$ was constrained as 10° away from being staggered and τ as 2° in such a direction as to decrease steric interactions between SiMe_3 groups on the same ligand.

Nonrefined RMS amplitudes of vibration were taken from Fjeldberg's study of $\text{HN}(\text{SiMe}_3)_2$ ¹⁹ or from the Mg^2 or Zn^3 bis(trimethylsilyl)amide study.

The four bond distances, three valence angles, dihedral angle $\phi(\text{N-Si})$, ten vibrational amplitudes for $M = \text{Fe}$, and nine amplitudes for $M = \text{Mn}$ and Co were refined under the constraints of a geometrically consistent r_a model. The best values obtained are listed in Table I. The quoted esd's have been multiplied by a factor of 3 to compensate for uncertainty due to data correlation and unrefined parameters.

The R factors, $R = [\sum w(I_{\text{obsd}} - I_{\text{calcd}})^2 / \sum w I_{\text{obsd}}^2]^{1/2} \times 100$, were 4.7% (Mn), 4.3% (Fe), and 5.6% (Co). The molecular intensities of the three

**Figure 1.** Molecular model of $M[N(\text{SiMe}_3)_2]_2$ ($M = \text{Mn, Fe, Co}$), with symmetry S_4 .

compounds are very similar. The Figure 2 we show the molecular intensities and the residuals for the compound with the poorest fit (Co). Experimental radial distribution (RD) curves are shown in Figure 3.

Photoelectron Spectroscopy. He I and He II photoelectron (PE) spectra of $M[N(\text{SiMe}_3)_2]_2$ ($M = \text{Mn, Fe}$) were determined by using a PES Laboratories 0078 PE spectrometer interfaced with a Research Machines 380Z microprocessor. The compounds were held at 45°C (Mn) and 40°C (Fe) during data acquisition. The spectra were calibrated with N_2 , Xe, and He.

The spectra are shown in Figures 4 and 5. The points give the experimental data, and the solid line represents a least-squares fit to these points. The notation of the bands follows that used previously.¹⁶ Ioni-

(18) Schäfer, L.; Yates, A. C.; Bonham, R. A. *J. Chem. Phys.* **1971**, *55*, 3055.

(19) Fjeldberg, T. *J. Mol. Struct.* **1984**, *112*, 159.

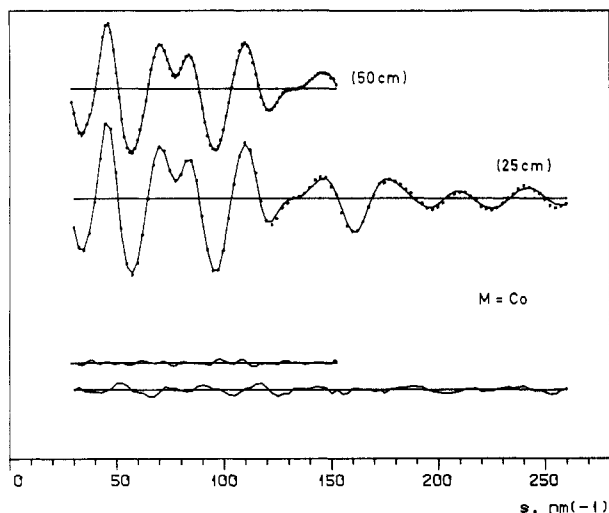


Figure 2. Modified molecular intensity curves and difference curves for $\text{Co}[\text{N}(\text{SiMe}_3)_2]_2$.

Table III. Total Energies, Orbital Energies, and Population Parameters Obtained by SCF MO Calculations on High-Spin (6A_1) $\text{Mn}(\text{NH}_2)_2$

Total Energies			
$R(\text{Mn-N})/\text{pm}$	energy/au	$R(\text{Mn-N})/\text{pm}$	energy/au
185	-1260.5694	195	-1260.5745
190	-1260.5742		

$R_c(\text{interpolated}) = 193 \text{ pm}$

Orbital Energies for $R = 190/195 \text{ pm}$			
orbital	ϵ/eV	orbital	ϵ/eV
5E	N(lone pair) -8.69/-8.54	4E	Mn(d π) -15.21/15.50
6B ₂	$\sigma(\text{Mn-N})$ -10.56/-10.44	5B ₂	Mn(d δ) -16.04/-16.27
7A ₁	$\sigma(\text{Mn-N})$ -12.77/-12.51	1B ₁	Mn(d δ) -16.04/-16.27
6A ₁	Mn(d σ) -13.01/13.50		

Orbital Populations			
Mn(4s)	0.51/0.50	Mn(total d)	5.13/5.13
Mn(d π)	1.02/1.02		

Net Charges			
Mn	+1.48/+1.49	H	+0.27/+0.26
N	-1.27/-1.27		

zation energies of the principal features and the proposed assignments are given in Table II.

Molecular Orbital Calculations. Ab initio molecular orbital calculations on high-spin 6A_1 (d^5) $\text{Mn}(\text{NH}_2)_2$ were carried out with the program DISCO²⁰ with a Gaussian type basis. We used for Mn a (12s, 6p, 4d) basis²¹ contracted to (9s, 4p, 3d), for N a (7s, 3p) basis²² contracted to (4s, 2p), and for H a (3s) basis²³ contracted to (2s).

$\text{Mn}(\text{NH}_2)_2$ was assumed to have D_{2d} symmetry. The N-H bond distance was fixed at 98 pm, $\angle\text{HNH}$ at 120° , and calculations were carried out at Mn-N bond distances of 185, 190, and 195 pm. The resulting energies are listed in Table III. Interpolation yields an optimal M-N bond distance of 193 pm.

The energies of the highest occupied molecular orbitals, some orbital occupancies, and net atomic charges obtained by population analysis are listed in Table III.

Results and Discussion

Mass spectra indicate that the three amides, $\text{M}[\text{N}(\text{SiMe}_3)_2]_2$ ($\text{M} = \text{Mn}, \text{Fe}, \text{Co}$) are monomeric in the gas phase. The gas electron diffraction data are consistent with molecular models in which the $\text{Si}_2\text{NMNSi}_2$ backbones have D_{2d} symmetry (and $\angle\text{NMN} = 180^\circ$) as indicated by a distinct peak at about 555 pm in the radial distribution curves, attributed to four equal, or nearly equal,

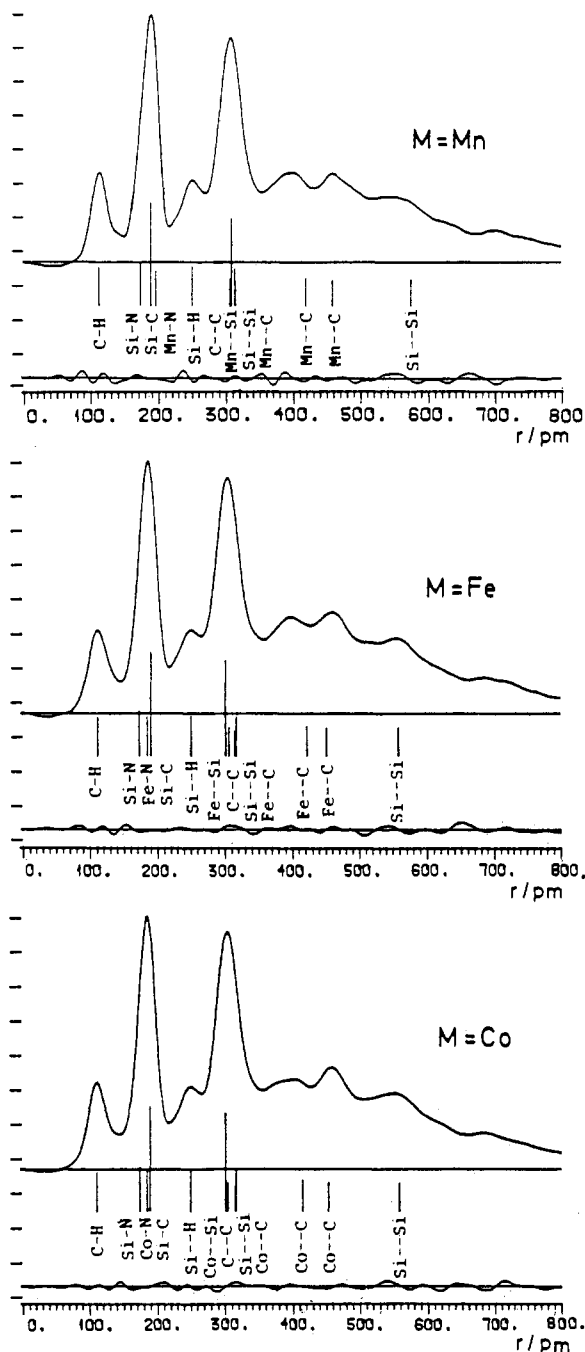


Figure 3. Experimental radial distribution curves and difference curves. The artificial damping constant $k = 20 \text{ pm}^2$.

interligand Si...Si distances. Molecular models of overall D_{2d} symmetry are not in agreement with the GED data; such models also lead to prohibitively short Me...Me contacts between SiMe_3 groups in the same ligand. The GED data are, however, in agreement with molecular models of S_4 symmetry obtained by rotating the Me_3Si groups by an angle $\phi(\text{Si-N})$ away from the D_{2d} conformation in such a way as to relieve the strain: $\phi(\text{Si-N}) = 17(1)^\circ$ ($\text{M} = \text{Mn}$), $13(1)^\circ$ ($\text{M} = \text{Fe}$), and $18(2)^\circ$ ($\text{M} = \text{Co}$).

Other structure parameters obtained by least-squares refinements are listed in Table I along with the corresponding parameters of the Zn analogue.³ The three amides for $\text{M} = \text{Fe}, \text{Co}$, and Zn are clearly very similar; no significant differences are found, not even between the M-N bond distances! It is, of course, disappointing that the M-N bond distances are determined with such low accuracy. The reason is that they are close to and hence strongly correlated with the Si-C bond distance ($\rho = -0.8$). When Si-C and Si-N are constrained to the values obtained for the Zn amide, we obtain Fe-N = 185 (1) and Co-N = 184 (1) pm.

(20) Almlöf, J.; Faegri, K., Jr.; Korsell, K. *J. Comput. Chem.* **1982**, *3*, 385.

(21) Roos, B.; Veillard, A.; Vinot, G. *Theor. Chim. Acta* **1971**, *20*, 1.

(22) Roos, B.; Siegbahn, P. *Theor. Chim. Acta* **1970**, *17*, 209.

(23) Duijneveldt, F. B. Technical Research Report No. RJ-945; IBM Corp.: Armonk, NY, 1971.

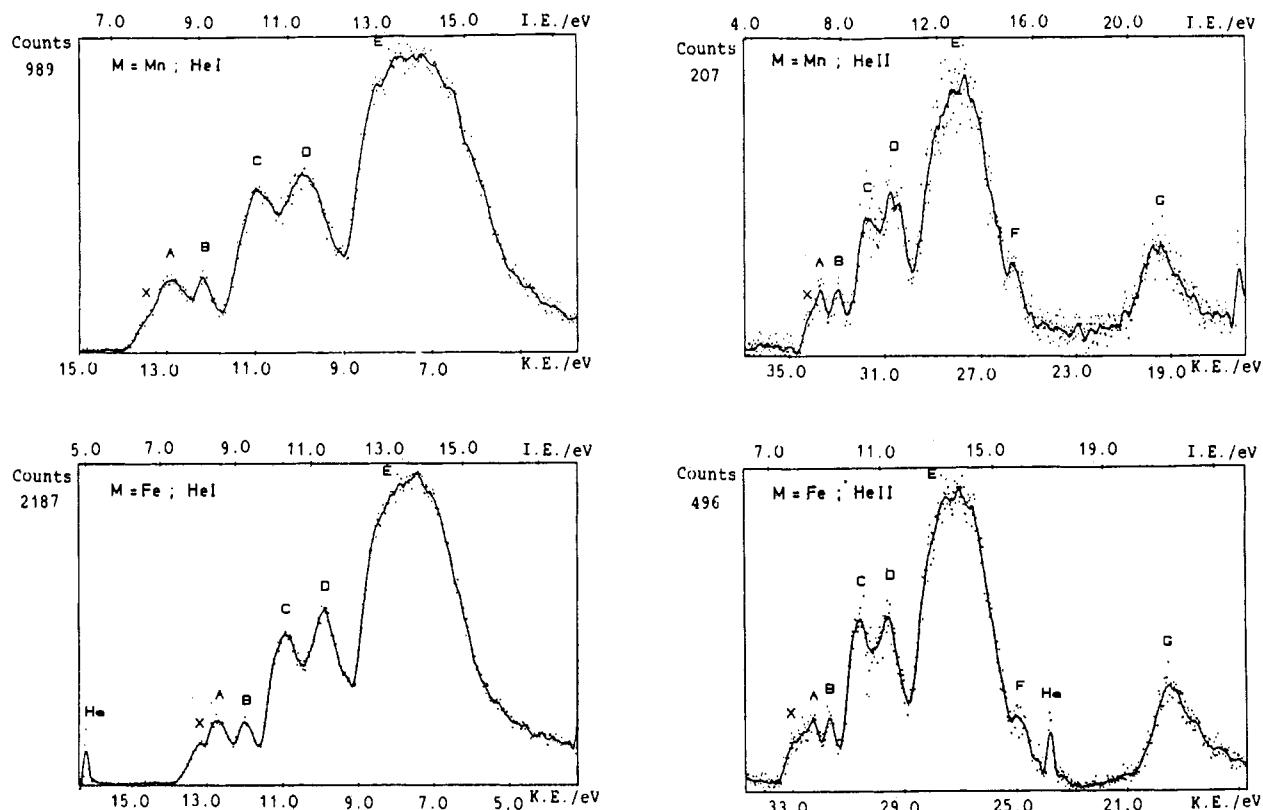


Figure 4. He I and He II spectra of $M[N(\text{SiMe}_3)_2]_2$ ($M = \text{Mn}, \text{Fe}$).

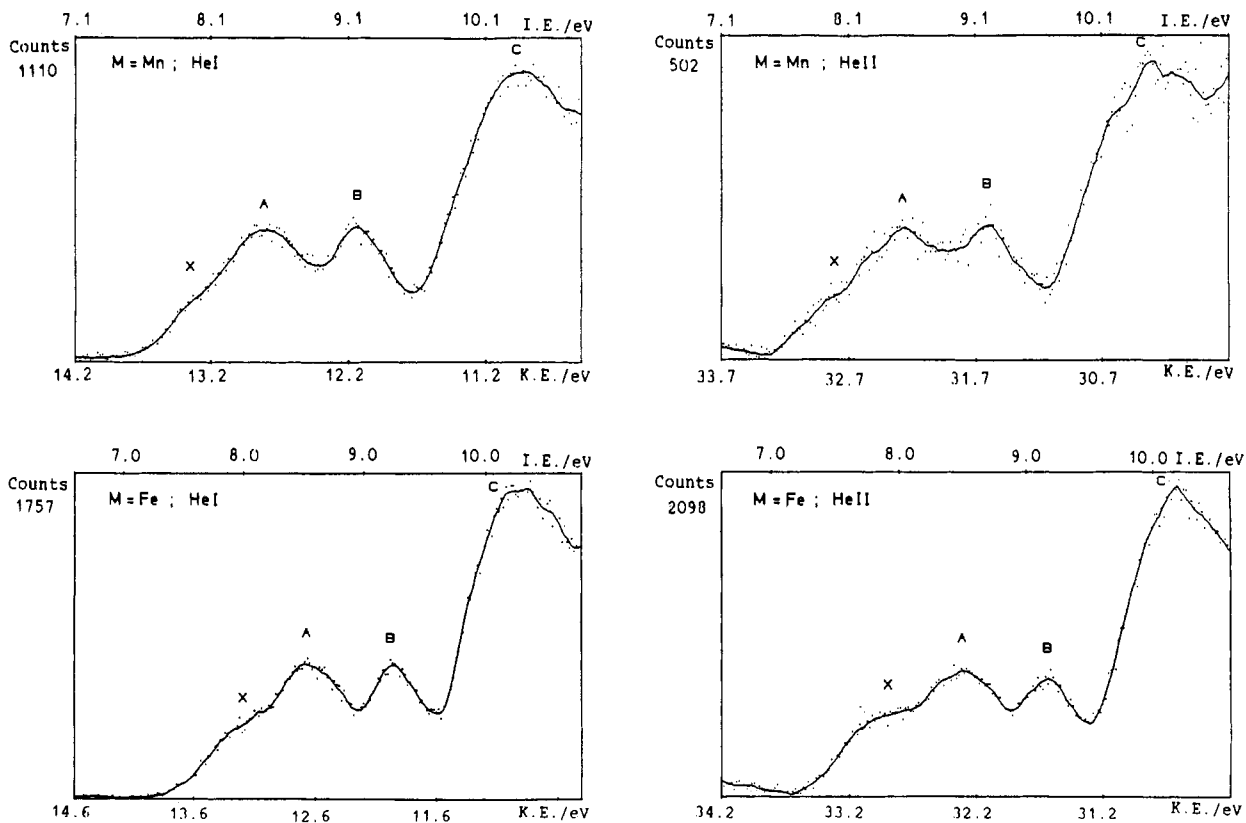


Figure 5. Low ionization energy regions of the spectra in Figure 4.

The M–N bond distance in $\text{Mn}[N(\text{SiMe}_3)_2]_2$, 195 (2) pm, is significantly longer than in the three other amides, but the structure of the ligand appears to be unaltered.

The N–Si and Si–C bond distances and the valence angles SiNSi and NSiC in the four amides are similar to those of the parent amine, $\text{HN}(\text{SiMe}_3)_2$.¹⁹ The wide SiNSi angles, 131.5 (1.5°) in $\text{HN}(\text{SiMe}_3)_2$,¹⁹ are probably another manifestation of

repulsion between the sterically demanding SiMe_3 groups.

The staggered equilibrium conformation might be due to weak dative $p\pi-d\pi$ bonding between N and the metal. A staggered conformation is, however, strongly favored by *interligand* interactions: in this conformation the shortest *interligand* C---C distances are of the order of 500 pm or greater, while rigid rotation into an eclipsed backbone conformation would lead to *interligand*

C...C contacts of 300 pm or less.

The molecular structure of the 1:1 complex of the Co amide with triphenylphosphine has been determined by X-ray diffraction.²⁴ In $\text{Co}[\text{N}(\text{SiMe}_3)_2]_2\text{PPh}_3$ the SiNSi angles are reduced by about 6° to $124(1)$ and $125(1)^\circ$. We interpret this compression of the ligands as evidence for interligand repulsion accompanying the introduction of a third bulky ligand at the metal atom. In the phosphine complex the Co-N bond distances have been increased by about 8 pm to 192(1) and 193(1) pm. The elongation may in part be due to interligand repulsion and in part to a reduced positive charge on the Co atom.

The Mn and Co amides are dimeric in the solid phase.^{12,13} On formation of a dimer the SiNSi valence angles in the terminal amide groups are reduced by about 10° to 121° (Mn) and 119° (Co), and the terminal M-N distances are increased by about 5 and 8 pm, respectively, to $\text{Mn-N}_t = 200$ pm and $\text{Co-N}_t = 192$ pm. Again, we interpret the compression of the ligand as evidence for congestion around the three-coordinate metal atoms and the stretching of the M-N_t bonds as being in part attributable to the same cause.

The bridging M-N distances, $\text{Mn-N}_b = 217$ pm and $\text{Co-N} = 200$ pm, are about 22 pm greater than in the monomers. These bonds are expected to be considerably longer than the covalent bonds of the monomers. The SiNSi angles in the bridging amido groups are reduced by nearly 20° to 112° (Mn) and 113° (Co).

While the Co amide is monomeric in freezing benzene,¹⁴ we find that the Mn amide is dimeric in pentane at room temperature. The Co amide is also the more volatile. Clearly the Co dimer is less stable with respect to dissociation than the Mn dimer. The difference may, at least in part, be due to greater congestion in the Co amide where the M-N distances are shorter and the ligands consequently are more tightly packed.

Magnetic susceptibility measurements on the three solid compounds from 5 to 290 K show very similar temperature dependencies. They do not follow the Curie-Weiss law, and at higher temperatures the magnetism becomes temperature independent. At 282 K and 5-kG field strength the magnetic moments are $\mu = 3.26$ ($M = \text{Mn}$), $\mu = 3.52 \mu_B$ ($M = \text{Fe}$), and $\mu = 5.08 \mu_B$ ($M = \text{Co}$) per monomeric unit. We interpret this to mean that the Fe amide is dimeric in the solid state, like the Mn and Co analogues, and that high-spin M^{2+} units are coupled in the dimers. A full account of the magnetic susceptibility studies will be published later.

The spin states of the monomeric units are, strictly speaking, unknown. In a high-spin (6A_1) Mn(II) amide each 3d orbital contains one electron. In a linear field the 3d orbital energies will increase in the series $d\delta < d\pi < d\sigma$. The D_{2d} symmetry of the $\text{Si}_2\text{NMNSi}_2$ backbone will remove the degeneracy of the $d\delta$ orbitals: $d\delta \rightarrow dB_1$ and dB_2 .

Since permutation of the five electrons between the d orbitals yields only one 6A_1 state, the high-spin amide may be assumed to be adequately described within the Hartree-Fock approximation. Ab initio MO calculations on high-spin $\text{Mn}(\text{NH}_2)_2$ yielded an optimal Mn-N bond distance of 193 pm. CASSCF calculations on the doublet states 2B_2 and 2E , which will not be reported in detail, indicated that these states are 500 kJ mol^{-1} higher in energy and that the Mn-N bond distance is 188 pm in both.

Experimentally, the bonding radius of high-spin Mn(II) is often found to be similar to that of Mg(II), while the low-spin bonding radius is shorter by 10 pm or more. The M-N bond distance in $\text{Mg}[\text{N}(\text{SiMe}_3)_2]_2$ is 191(3) pm.² We conclude that the monomeric Mn amide is high spin in the gas phase.

Before proceeding, we pause to note that the results of population analysis (Table III) suggest that the Mn-N bonds are very polar, $Q(\text{Mn}) = +1.27$, and that $p\pi-d\pi$ bonding is negligible.

We now turn our attention to the PE spectrum of $\text{Mn}[\text{N}(\text{SiMe}_3)_2]_2$. The spectrum is readily assigned by comparison with

those of other[bis(trimethylsilyl)amido]metal compounds; see Table II. Band A at 8.5 eV is assigned to ionization from the N lone pairs. The MO calculation on $\text{Mn}(\text{NH}_2)_2$ yields the degenerate N lone pair orbitals as the highest occupied MO with an energy of about -8.6 eV. Band B is assigned to ionization from the Mn-N σ -bond orbitals. The MO calculations yielded the orbital energies -10.7 eV ($6B_2$) and -13.0 eV ($7A_1$). The latter orbital is more metal centered than the former, and ionization from this orbital will be accompanied by greater relaxation in the ion. The energies of ionization from these two orbitals may therefore be close enough for them to give rise to one band. Alternatively the band corresponding to ionization from the A_1 Mn-N orbital may fall under band C. The higher energy bands are all assigned to ligand-centered orbitals.

The low-energy shoulder X at about 7.9 eV, which increases in relative intensity in the He II spectrum, is assigned to ionization from the $3d\sigma$, which according to ligand field theory is the highest of the d orbitals; ionization bands from the other 3d orbitals are presumably concealed beneath bands A and B.

With our assignment, the observed ionization energies increase in the order $3d\sigma < \text{N}(\text{lone pair}) < \sigma(\text{M-N})$. This is different from the order predicted by application of Koopmans' theorem to the calculated orbital energies of $\text{Mn}(\text{NH}_2)_2$: $\text{N}(\text{lone pair}) < \sigma(\text{M-N}) < 3d\sigma$. The reason for the discrepancy may be that the ordering of the energy levels is changed when the four H atoms in $\text{Mn}(\text{NH}_2)_2$ are replaced by SiMe_3 groups. It is also possible that the energy gained through relaxation of the molecular ion is greater when ionization has occurred by removal of an electron from the metal-centered $3d\sigma$ orbital.

The PE spectra of the Fe and Co amides are very similar to that of the Mn analogue and may be similarly assigned. Band X may be assigned to ionization from $d\sigma$ in high-spin species or $d\pi$ (dE) in low-spin species. The lack of detailed d band structure precludes firm conclusions about the spin states, but the similarity of the spectra does suggest that the gas-phase monomers all are high spin, like the solid-phase dimers.

The additional electrons in the Fe amide and Co amide would then reside in the ligand-field-stabilized $d\delta$ (dB_1 and dB_2) orbitals, and M-N bond distances would be expected to decrease in the order $\text{Mn-N} > \text{Fe-N} > \text{Co-N}$. The Fe-N distance is in fact found to be $\Delta r = 11(3)$ pm shorter than the Mn-N distance, but the Fe-N and Co-N bond distances are indistinguishable within their large combined uncertainty ($\Delta r = 0(3)$ pm). In this connection it may be pertinent to point out that the higher ionization energy from the M-N σ -bonding orbitals (band B) in the Co compound suggests that M-N bonding is stronger in this compound than in the other two.

The Fe-N bond distance of the gaseous bis(amide), 184(2) pm, is significantly shorter than that of the crystalline tris(amide), $\text{Fe}[\text{N}(\text{SiMe}_3)_2]_3$, 191.7(4) pm by X-ray crystallography.²⁵ The tris(amide) is known to be high spin.²⁶ Normally the bonding radius of the metal is expected to decrease with increasing oxidation state.

The anomaly may, at least in part, be due to stretching of the M-N bonds in the Fe(III) amide due to interligand repulsion; the strain is clearly indicated by a relatively narrow SiNSi angle, $121.2(4)^\circ$. The anomaly would, of course, be removed if the Fe(II) amide is found to be low spin.

Acknowledgment. The work at Berkeley was supported by the University of California Committee of Research, the work at Brighton and Oxford by the SERC, and the work at Oslo by the Norwegian Research Council for Science and the Humanities.

Registry No. $\text{Fe}[\text{N}(\text{SiMe}_3)_2]_2$, 14760-22-6; $\text{Co}[\text{N}(\text{SiMe}_3)_2]_2$, 14760-23-7; $\text{Mn}[\text{N}(\text{SiMe}_3)_2]_2$, 926-76-1; $\text{FeBr}_2(\text{THF})_2$, 70317-91-8; $\text{Mn}(\text{N-H}_2)_2$, 100408-78-4.

(24) Bradley, D. C.; Hursthouse, M. B.; Smallwood, R. J.; Welch, A. J. *J. Chem. Soc., Chem. Commun.* **1972**, 872.

(25) Bradley, D. C.; Hursthouse, M. B.; Rodesiler, R. F. *J. Chem. Soc., Chem. Commun.* **1969**, 14.

(26) Aleya, E. C.; Bradley, D. C.; Copperthwaite, R. G.; Sales, K. D. *J. Chem. Soc., Dalton Trans.* **1973**, 185.